PID Controller Design by Grasshopper Optimization Technique for Performance Enhancement of Hybrid Renewable Energy System

RITIKA ARORA
Amity University ,Uttar Pradesh, INDIA

VIJAY KUMAR TAYAL
Amity University, Uttar Pradesh, INDIA

HEMENDER PAL SINGH
Amity University,Uttar Pradesh, INDIA

SUKHBIR SINGH
MSIT Delhi, INDIA

Abstract: The conventional energy sources are depleting with rise in power demand day by day. The renewable energy sources may serve as promising solution towards present day energy crisis. They are pollution free, cheaper and abundantly available in nature. The frequently used wind and PV renewable energy sources are intermittent in nature. Due to uncertainties in wind speed, solar irradiation and loading conditions, there are large variations in peak overshoot, settling time and total harmonic distortion (THD) of output power. This paper describes dynamic modeling and PID control design for hybrid renewable energy system with wind, photovoltaic and fuel cell. The PID controller is used to obtain the constant AC output from the hybrid system integrated with grid. To yield the better output, the Grasshopper optimization algorithm (GOA) tuned the PID controller parameters. The simulation results of proposed hybrid system show a remarkable improvement in peak overshoot, settling time and total harmonic distortion (THD).

Keywords: Hybrid energy system, renewable energy system, Grasshopper optimization technique, Dynamic modeling of hybrid system.

1. Introduction

The conventional power sources are depleting very speedily. Increasing consumption, high costs, exhausting nature of fossil fuels and high emissions have created the need to invest in renewable resources of energy. These energy sources are environment friendly, less noisy and pollution free. The most commonly used renewable energy sources are solar and wind. The variable wind speed of wind turbine creates fluctuations in output power. To overcome this issue, power converters and proper control strategies is used in wind power hybrid generation.

Many researches on hybrid power generation system using renewable energy sources [1-5] includes modeling of different components. Most researches include the optimization of MPPT strategies [6]. The authors described the real time energy management of wind - micro turbine energy system. Eskander et al. [7] describes the fuzzy control strategy for MPPT of wind and PV system. The P&O algorithm for tracking wind mill power for 80W module has been proposed by Wang et al. [8]. To use PV and wind turbine as hybrid generation, some of the backup power is always required. Hongxing et al. [9] described application of large batteries

or super capacitors for hybrid generation with solar and wind. When solar and wind energy are abundant, energy can be stored and can be utilized later when there are peak periods, described by Mitchell et al. [10]. Tomonobu et al. [11] showed simulation output of hybrid system with electrolyzer fuel cell and distributed generation. The simulation of PV–fuel cell generation system and battery storage system was provided by Saiful and Ronnie [12]. The problem with battery is its charging and discharging cycle, causing battery to lose its capacity. The sizing optimization method [13-19] guarantees the full use and low investment of PV, Wind turbine and storage system for system that can work under optimum conditions for residential and commercial purposes. The hybrid system with Wind turbine, PV array and fuel cell has been described by Kaushik [20] to provide pollution less, high efficiency diversity of fuels, heat reusability in comparison to conventional huge lead-acid batteries.

In literature, various artificial intelligence techniques such as genetic algorithm (GA), particle swarm optimization (PSO), ant colony optimization (ACO) [21-24] etc. have been proposed by the researchers. However, GA suffers from the problem of convergence. The problem associated with PSO is its slow convergence and they fall into local optimum in high dimensional space. The ACO has probability distribution problem that can change for every iteration. In this paper, PID control design for a hybrid power system model comprises of wind mill, fuel cell and solar array subjected to an uncertain load is presented. The PID controller parameters are tuned using grasshopper artificial intelligence technique. The main advantage of GOA is that the local optima is avoided with ability to achieve the global optima in given space. The incremental conductance algorithm is used to track the maximum power from the sun. The simulations of proposed hybrid power systemare carried out using MATLAB. The comparison of system with PID controller and GOA optimized PID controller shows great performance enhancement of output power. This paper is organized as follows – section 2 elaborates the hybrid system description, the control strategy along with Grasshopper optimization algorithm is discussed in section 3, Matlab model of the hybrid control system with controller is presented in section 4, section 5 discusses the simulation results and conclusion is presented in section 6.

2. Hybrid System Description

The Hybrid power generation system consist of (a) wind energy system (b) PV array and (c) Fuel Cell stack is described in Figure 1. The obtained variable DC is converted into constant DC by means of boost/buck-boost converters. This DC is converted into 3 phase AC by IGBT inverter for connection to Grid and load. The IGBT inverter gating pulses are obtained from PID controller. The PID controller parameters are tuned using Grasshopper optimization algorithm.

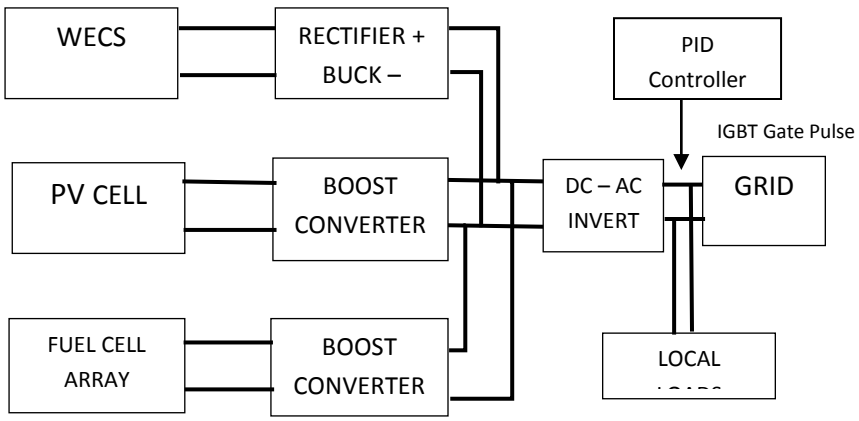

Figure 1: Block diagram of Proposed Hybrid System

2.1. Wind Energy Conversion System

Wind is most abundantly available renewable energy sources. Several studies [25-28] have been done on wind turbine and generators. Wind rotates the blades of the turbine which in turn rotates the alternator delivering AC power output.
The wind's output power [29-30] is given by the equation (1):

$$Pm = \frac{1}{2}\,\rho\, A\, C_p v^3 \tag{1}$$

Where, A –Turbine covered area (m^2)
C_p - Power coefficient of the wind turbine
v – Wind speed (m/sec)
ρ – Air density (Kg/m^3)

If wind speed, swept area and air density is constant, the output power will be a function of power coefficient of turbine. The wind turbine is identified by its $C_p - \lambda$ curve [Figure 2], where λ is tip speed ratio as given in equation (2)

$$\lambda = \omega R/V \tag{2}$$

Where, ω -Rotor speed of turbine (rad/sec)
R - Turbine blade radius (m)
V - Wind speed (m/sec)

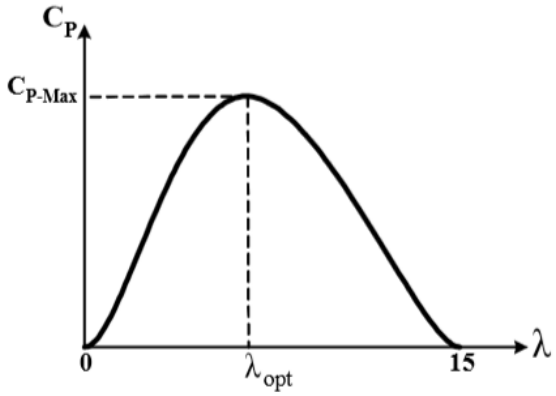

Figure 2: Power Coefficient vs. Tip-Speed Ratio

Figure 2 shows the λ_{opt} point corresponding to the maximum value of Cp. At this point, the optimum efficiency is obtained with the maximum output power by wind generator.
Figure 3 shows the power output of the wind turbine and rotor speed corresponding to different wind speeds such that $V_3 > V_2 > V_1$. This has been observed that at V_1 speed, maximum power is obtained at ω_1 rotor speed, at an operating point denoted by A. On changing wind speed from V_1 to V_2, the operating point at ω_1 is shifted to B. However, at this point,the power output is not the maximum. To obtain the maximum power at V_2, the speed must be elevated to ω_2 corresponding to operating point C.

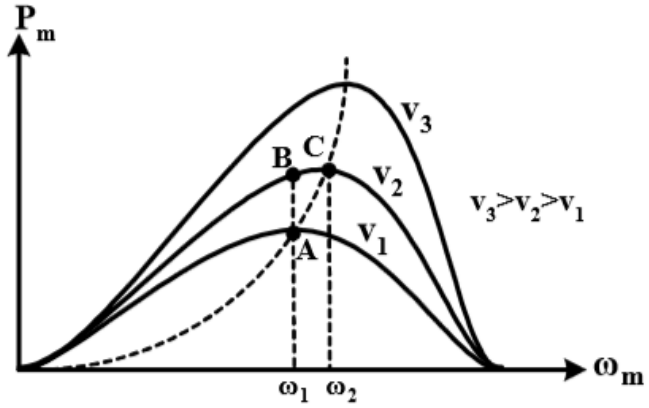

Figure 3: Output Power vs. Rotor Speed

The optimum speed is mathematically given by:

$$\omega_{opt} = \frac{v.\lambda_{opt}}{R} \rightarrow v = \frac{R.\omega_{opt}}{\lambda_{opt}} \quad (3)$$

The output power of turbine can be obtained by substituting wind speed from equation (3) into (1):

$$P_m = \frac{1}{2}\rho A C_p \left(\frac{R.\omega_{opt}}{\lambda_{opt}}\right)^3 \quad (4)$$

The torque can be obtained as:

$$T_{target} = k_{opt} \cdot {\omega_{opt}}^2 \quad (5)$$

Where, $k_{opt} = \frac{1}{2}\rho A C_{pMax}\left(\frac{R}{\lambda_{opt}}\right)^3$

2.2. Photovoltaic power generation System

The solar cell is the most basic element of a Photo Voltaic array. This generates DC electric power from solar radiations. Due to variations in intensity of solar irradiation throughout the day, the output DC power is fluctuating. Thus DC to DC converter is required to regulate the obtained DC power.

The basic principle to generate the power through solar cell (Patel [31]) is similar to p-n junction diode. The relation of output voltage and load current [32-33] is given by equation (6):

$$I = I_L - I_0\left[exp\left(\frac{V+IR_S}{\alpha}\right)t\right] \quad (6)$$

Where, I_L – Light Current (A)
I_0 – Diode reverse saturation Current (A)
I – Load Current (A)
V – Output voltage (Volts)
R_S – Series Resistance of PV cell (ohms)
α – Thermal voltage timing completion factor of cell (volts)

Figure 4 Showsthe V-I characteristics of PV stack (operating at standard irradiance of 1000 W/m^2 at 25^0).

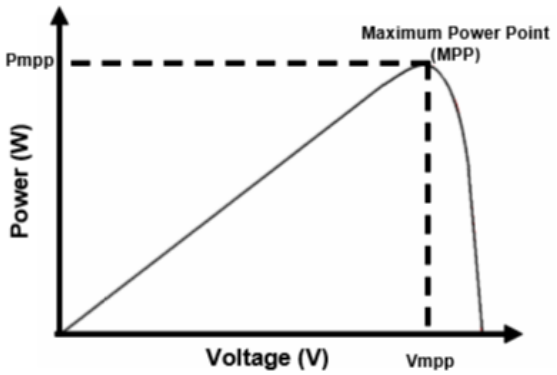

Figure 4: Power –Voltage (PV) Characteristics of a photovoltaic array

If the irradiance level is varied from 1000 W/m^2 to 600 or 400 W/m^2, then PV characteristics changes as shown in Figure 5. This has been observed that the low irradiation yields in low value of maximum output power obtained from PV arrays.

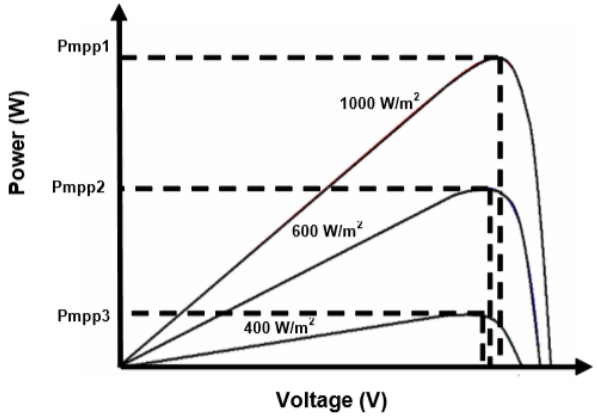

Figure 5: P-V Characteristics of Photovoltaic Array for different Irradiation levels

2.3. Fuel Cell Stack System

The chemical device in which chemical reaction generates the electricity is named as fuel cell.A fuel cell has two electrodes namely cathode and anode, and an electrolyte. The electrodes and electrolyte materials are not altered in this process. Byproducts obtained are only water and heat if the fuel is pure hydrogen. The advantages of fuel cell are that no moving part is available, low cost and no gaseous emission. Various types of fuel cells such as – Proton Exchange Membrane (PEM) fuel cell, Solid Acid (SA) fuel cell, Alkaline fuel cell (AFC) etc are available. The PEMFC is one of the most commonly used fuel cell due to following advantages - (i) Environment friendly (ii) Easier installation (iii) Simple mechanism of working (iv) Low maintenance required (v) Long life (vi) Low operating temperature (below 100˚C) and (vii) High efficiency. In this work, PEMFC is considered for hybrid renewable energy system.
In a PEMFC, polymer membrane is used as an electrolyte [34-35]. The air is used as an oxidant and hydrogen as a fuel at atmospheric pressure.
The typical reaction of fuel cell is given by:

$$H_2 + O_2 \rightarrow H_2O \quad (7)$$

Output terminal voltage [34] of fuel cell is given by equation (8):

$$V_{CELL} = E - \Delta V_{act} - \Delta V_{ohm} - \Delta V_{trans} \quad (8)$$

Where, E - Open circuit voltage

ΔV_{act}- Voltage drop due to cathode and anode's activation

ΔV_{ohm} - Ohmic voltage drop

ΔV_{trans} - Voltage drop of concentration of reactants gases

For each solar cell, considering the equivalent output voltage, the current for complete fuel cell stack can be calculated by equation (9):

$$V_{FC} = N_{CELL}\left[E - ln\left(\frac{I_{FC}+A_{CELL}i_n}{A_{CELL}i_o}\right) - r\left(\frac{I_{FC}}{A_{CELL}}\right) - m\,exp\left(n\frac{I_{FC}}{A_{CELL}}\right)\right] \quad (9)$$

Where, N_{CELL}- Cells connected in series

A_{CELL}- Area of electrodes

The total power of fuel cell can be given by the following equation:

$$P_{FC=}N_{CELL}\,.V_{CELL}\,.I_{FC}$$

(10)

Figure 6 Shows the V-I and P-I characteristics of fuel cell stack.

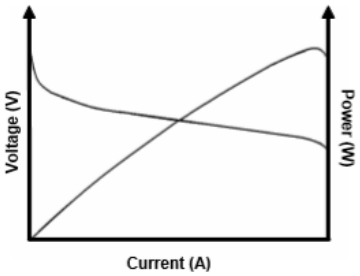

Figure 6: Voltage-Current (V-I) and Power – Current (P-I) Characteristics of Fuel Cell

3. Control Strategy

Because of variable and unforeseeable nature of wind and solar energy, the electric power generated is also variable. Figure 7 shows the simulink model responsible for tuning and stabilizing the DC voltage of the DC link. The desired D.C voltage is 800 volts. This voltage is fed as the reference voltage and subtracted from the current value of the DC voltage to get the error. The obtained error signal is given to the PID controller. Furthermore, PID controller decides the duty ratio of the IGBT of the to tune the Voltage level to its desired value. To achieve the best output the optimized parameter values of PID are identified by the Grasshopper Optimization Algorithm.

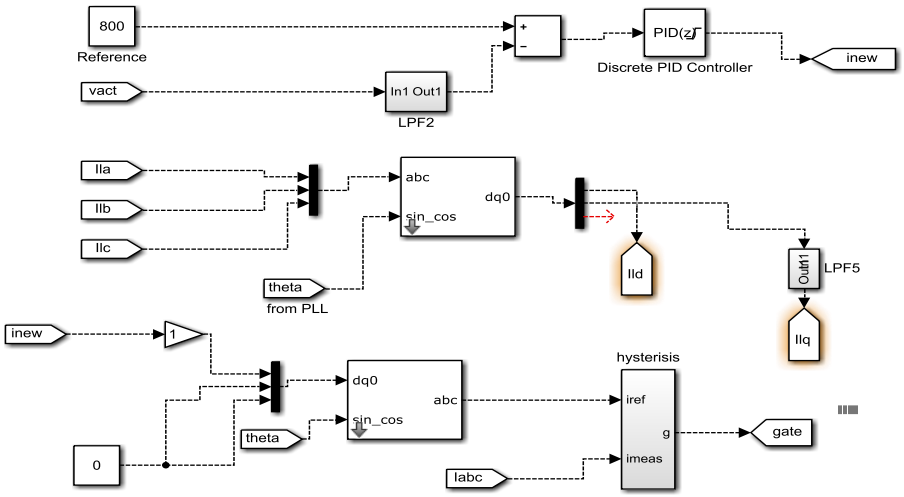

Figure 7: Control Strategy Simulink block

3.1. Grasshopper Optimization Technique

Optimization helps to achieve the best design for prioritized criteria or constrains [36]. The optimization can be single or multi objective for any specific problem [37-38]. Grasshopper Algorithm is one of the most efficient and latest artificial intelligence techniques.

Grasshopper optimization algorithm (GOA) is based on grasshopper's behavior for search of food. Grasshoppers (insects) are considered as pests as they cause harm to the crop and

agriculture. Usually grasshoppers are seen single but also found in large swarm. The swarming behavior can be found in both nymph and adulthood grasshoppers. Grasshoppers eat almost every vegetation coming in their path. In larva phase, swarm has very slow motion. While opposite is in adult hood, i.e. abrupt movement and long range of swarm. The exploration and exploitation are two main features of nature based algorithms [39-40].

A mathematical model for simulation of swarming behavior of grasshoppers is depicted as follows [41-42]:

$$X_i = S_i + G_i + A_i \tag{11}$$

Where, X_i – i[th] grasshopper's position

S_i – Social interaction

G_i – Gravity force on i[th] grasshopper

A_i - Wind advection

For random behavior of grasshoppers, equation can be manipulated as given by equation (12):

$$X_i = r_1 S_i + r_2 G_i + r_3 A_i \tag{12}$$

Where, r_1, r_2 , r_3 are random numbers in the range (0,1).

The S_i can be given by equation (13):

$$S_i = \sum_{\substack{j=1 \\ j \neq i}}^{N} s(d_{ij})\, \overrightarrow{d_{ij}} \tag{13}$$

Where d_{ij} provides the distance between i[th] and j[th] grasshopper and given as:

$$d_{ij} = |X_j - X_i| \tag{14}$$

S factor in the equation (13) provides social force's strength and $\overrightarrow{d_{ij}}$ is unit vector from i[th] to j[th] grasshopper:

$$\overrightarrow{d_{ij}} = \frac{X_j - X_i}{d_{ij}} \tag{15}$$

And s can be given by equation (16):

$$s(r) = f \cdot e^{-r/l} - e^{-r} \tag{16}$$

Parameter 'f' denotes the intensity of attraction and 'l' is attractive length scale. Function 's' shows the attraction or repulsion of grasshopper. Component G in equation (12) can be given as:

$$G_i = -g \cdot \overrightarrow{e_g} \tag{17}$$

Where, g is gravitational constant and $\overrightarrow{e_g}$ is the unit vector towards the center of earth.

Factor A can be calculated as:

$$A_i = u \cdot \overrightarrow{e_w} \tag{18}$$

Where u is constant drift and $\overrightarrow{e_w}$ is unity vector in the direction of wind.

The nymph grasshoppers don't have wings. Because of this, nymph's movement is highly correlated with wind's direction and can be described by equation (19):

$$X_i = \sum_{\substack{j=1 \\ j \neq i}}^{N} s\left(d_{ij}\right)\overrightarrow{d_{ij}} - g \cdot \overrightarrow{e_g} + u \cdot \overrightarrow{e_w} \tag{19}$$

N provides the number of grasshoppers. This equation provides the simulation of interaction between grasshoppers in the swarm. The mathematical modelling cannot be used directly for grasshopper swarm because they reach the comfort zone very quickly and do not cover the specific point. Therefore, a modified version of equation (19) is given by equation (20):

$$X_d^i = \left(\sum_{\substack{j=1 \\ j\neq i}}^{N} c\ \frac{U_{bd} - L_{bd}}{2}\ .\ s\ .\left(\left|X_j^d - X_i^d\right|\right)\frac{X_j - X_i}{d_d}\right) + T_d \quad (20)$$

Where, U_{bd} - upper bound in D^{th} dimension

L_{bd} – Lower bound in D^{th} dimension

T_d - Best solution obtained so far

C – Decreasing coefficient to the attraction, repulsion and comfort zone.

The main advantages of GOA are [43] - (i) Most promising region from given space can be found by grasshoppers (ii) Very accurate solution is obtained for unconstrained optimization problems (iii) GOA provides promising and correct results for constrained optimization problems and (iv) Local and global optima are obtained in given space.

Figure 8 shows the flow chart of the GOA algorithm. The initialization is done at the initial step thereafter random population is generated. Afterwards, fitness function for each population is evaluated. Then the updated parameters normalize the distance among the grasshopper. Further, update the positions and iterate the process for all the members of the population. Iterate the process and update the overall best solution.The optimization process is stopped if termination criteria is reached.

The Hybrid system with Wind-PV-Fuel cell combination is being optimized using GOA algorithm. The control strategy is to tune the PID controller values for obtain optimized output from the hybrid system in the presence of uncertainties in loading conditions. The DC link voltage is generally varying as the renewable energy generation is never constant. Figure 9 displays the flow chart of optimization of PID parameters i.e. K_p, K_i and K_d. The parameters of conventional PID and GOA-PID controllers are shown in Table 1.

Table 1: PID Controller parameters

Parameters	Conventional PID Values	GOA-PID Values
Kp	0.72	-0.92
Ki	0.08	0.17
Kd	0	0

4. MATLAB / SIMULINK Implementation of the Hybrid System

Mathematical models of wind turbine, PV array and fuel cell are shown independently in different figures. The overall Hybrid power generation model interfaced with different power electronic components and with grid connection with different AC loads is shown in Figure 10

.

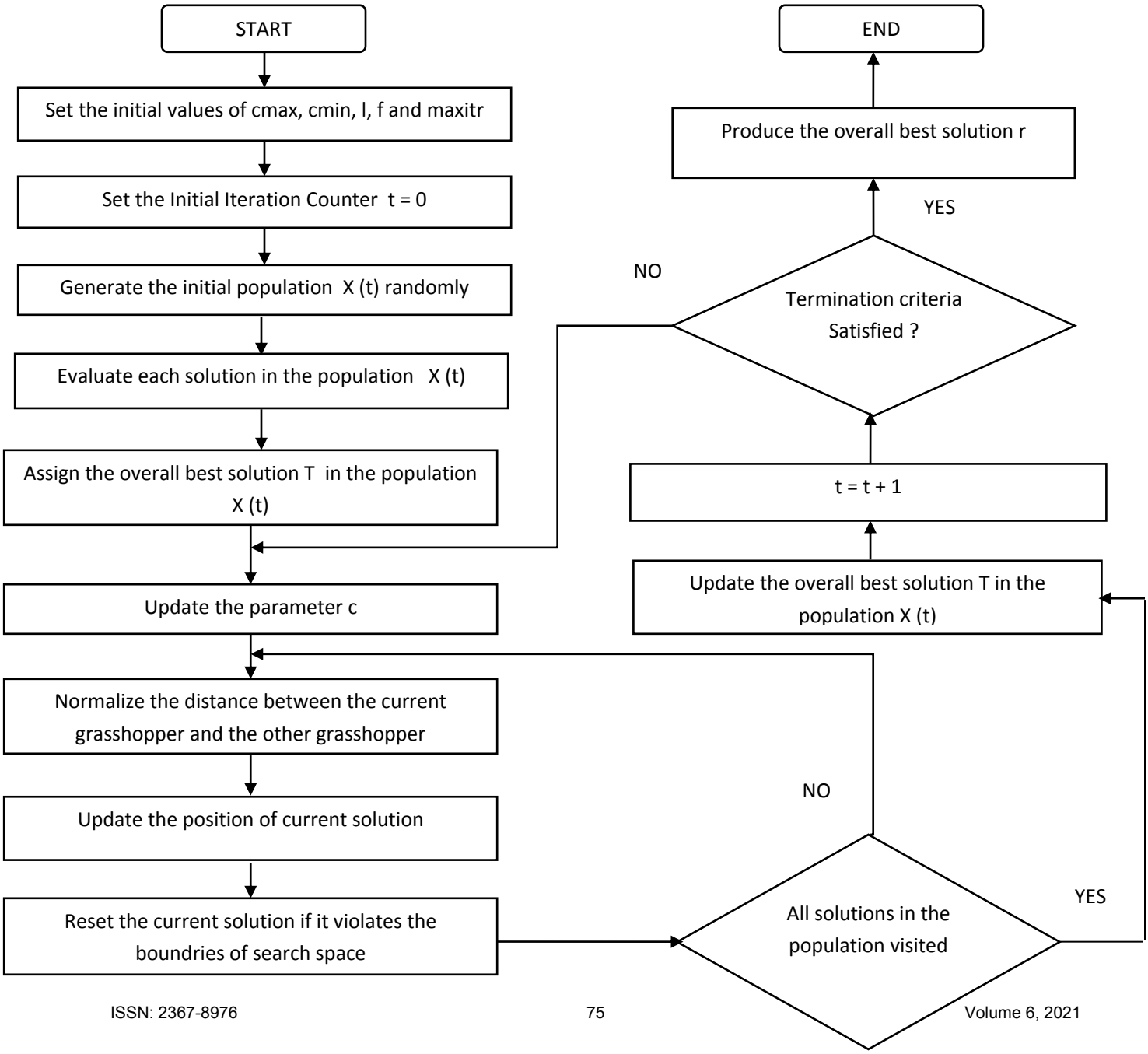
START
Set the initial values of cmax, cmin, l, f and maxitr
Set the Initial Iteration Counter t = 0
Generate the initial population X (t) randomly
Evaluate each solution in the population X (t)
Assign the overall best solution T in the population X (t)
Update the parameter c
Normalize the distance between the current grasshopper and the other grasshopper
Update the position of current solution
Reset the current solution if it violates the boundries of search space
All solutions in the population visited
NO
YES
Update the overall best solution T in the population X (t)
t = t + 1
Termination criteria Satisfied ?
NO
YES
Produce the overall best solution r
END

Figure 8: Flow Chart of GOA

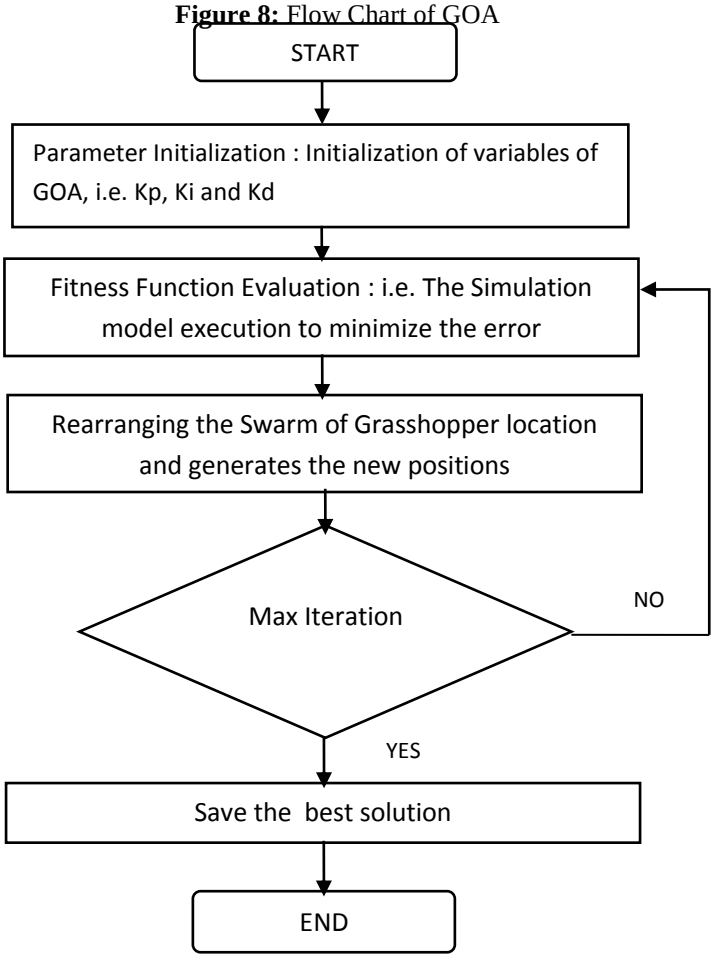

Figure 9: Flow Chart of The PID tuning using GOA

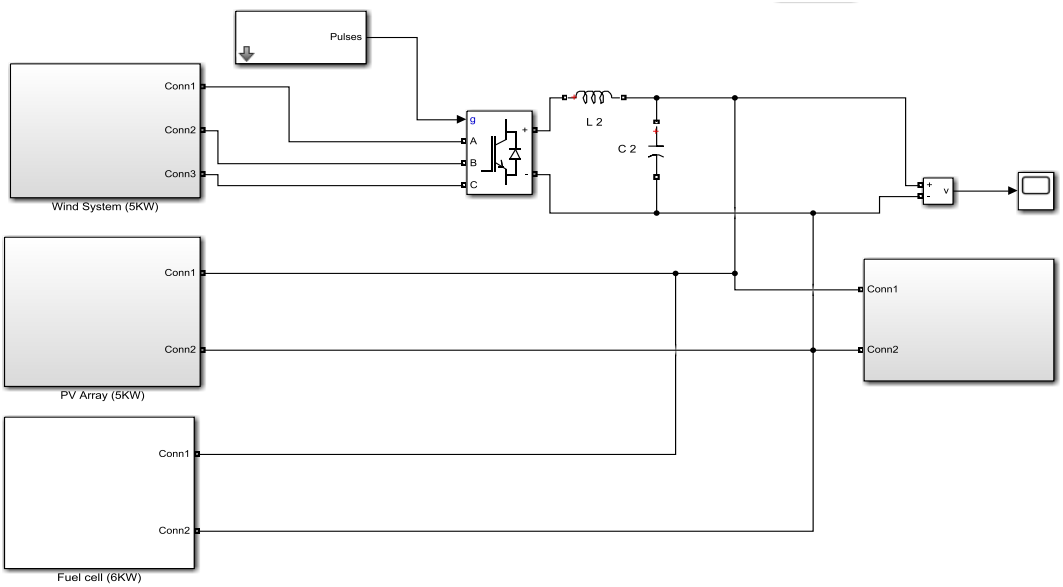

Figure 10: Wind-PV Array-Fuel Cell combined Matlab / Simulink Model

The Simulink model for wind turbine is presented in Figure 11.

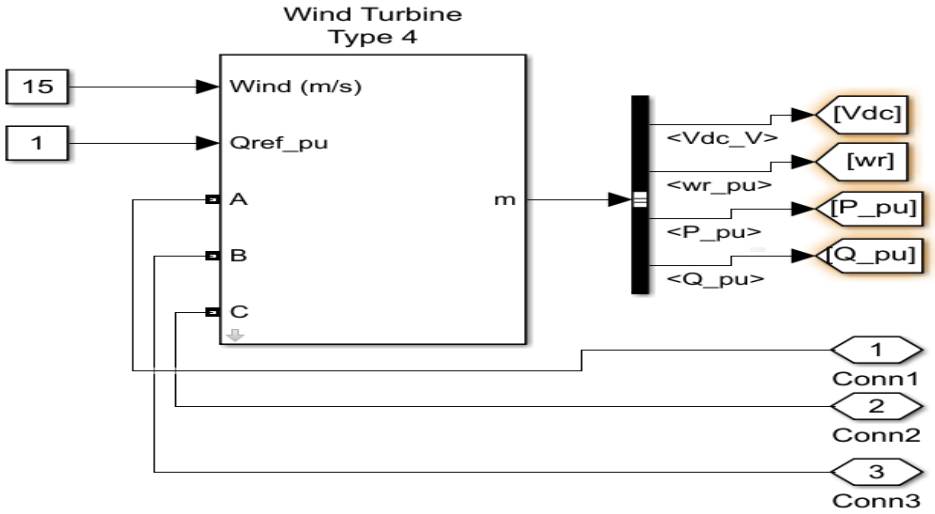

Figure 11: Wind Matlab/Simulink Model

The Simulink model for PV array is shown in Figure 12:

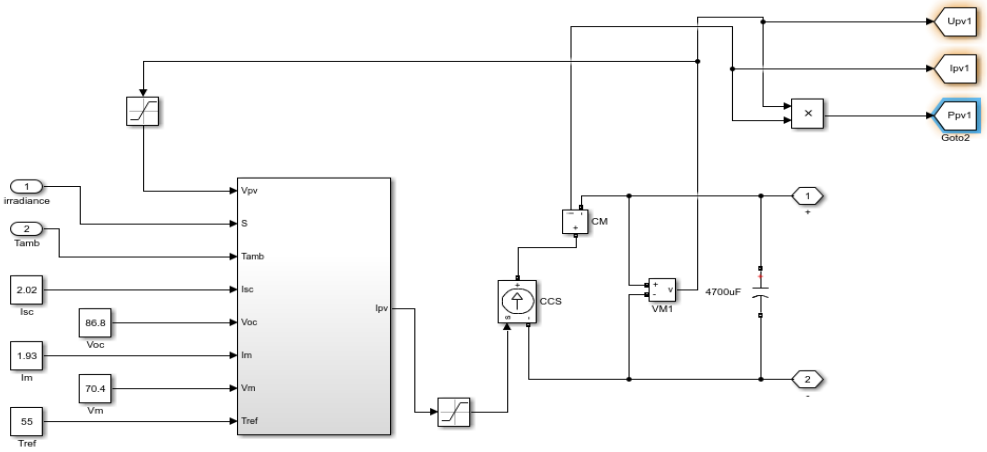

Figure 12: Photovoltaic Panel MATLAB / Simulink Subsystem

Simulink model for fuel cell stack is shown in Figure 13.

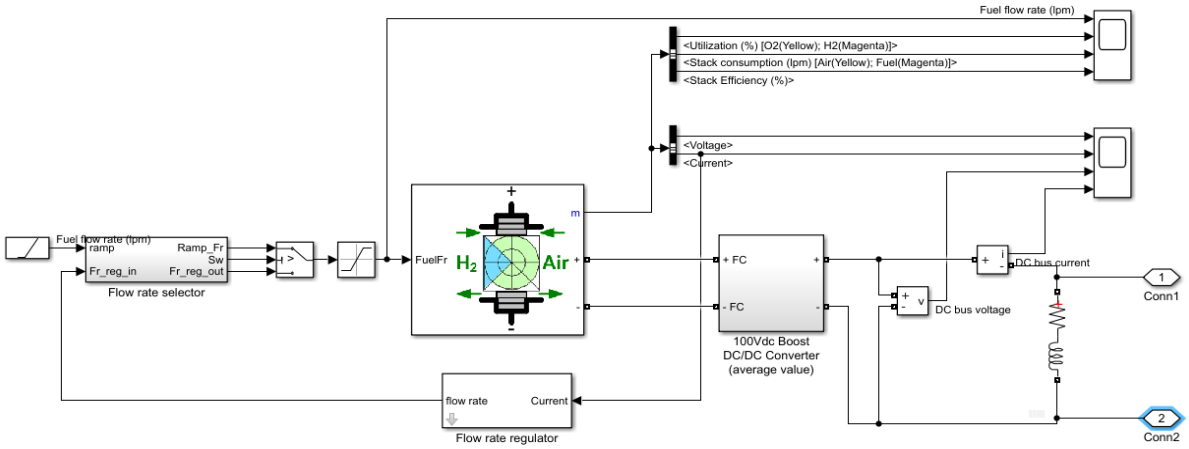

Figure 13: Fuel Cell MATLAB / SIMULINK model

5. Simulation Results

The proposed hybrid system comprised of PV, wind and fuel cell energy sources (Figure 10) is simulated with uncertain loading conditions. To judge the effectiveness of the proposed control scheme, R - L load has been suddenly reduced from 24KW to 12 KW at t = 0.5 sec and further increased to 24 KW at t = 0.7 sec. The maximum power output required from the system is 8 KW. The reference DC is 800 Volt. The gate switching of the IGBT inverter is controlled by the GOA tuned PID controller. Figure 14 shows the inverter DC input voltage with conventional PID and GOA-PID. From Figure it is shown that the overshoot (%) is decreased from 6.5 to 0.05 and settling time is reduced from 0.16 sec to 0.09 sec for PID controller and GOA optimized PID controller respectively also shown by Table 2.

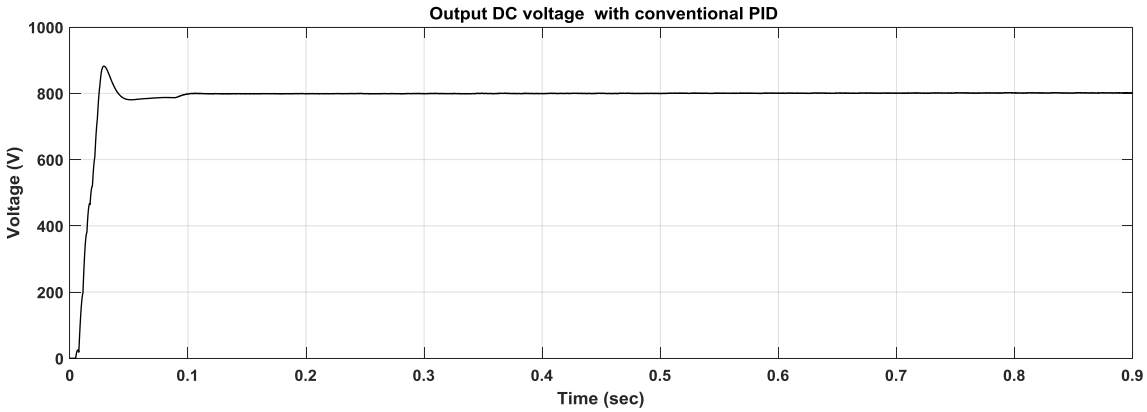

Figure 14 (a): Output DC voltage from hybrid renewable sources with conventional PID

Table 2: Comparison of Overshoot and Settling Time of Inverter DC Input Voltage

Parameter	**With PID Controller**	**With GOA-PID Controller**
Overshoot	6.5 %	0.05 %
Settling time	0.16 sec	0.09 sec

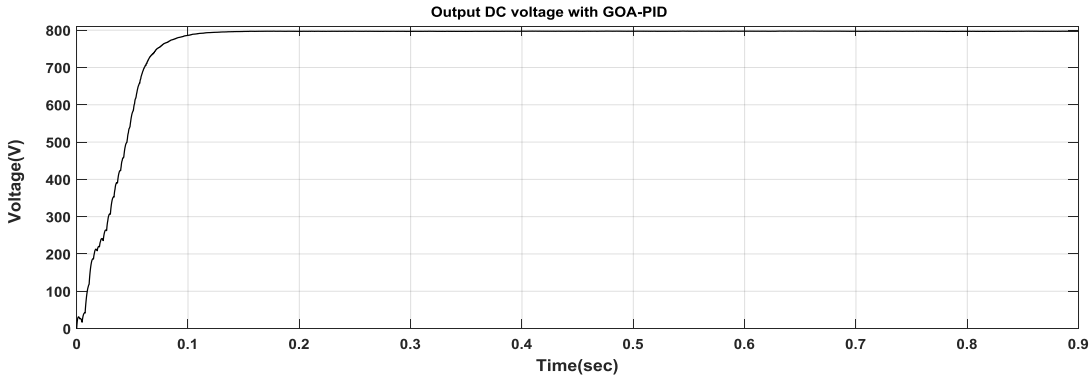

Figure 14 (b): Output DC voltage from hybrid renewable sources with GOA-PID

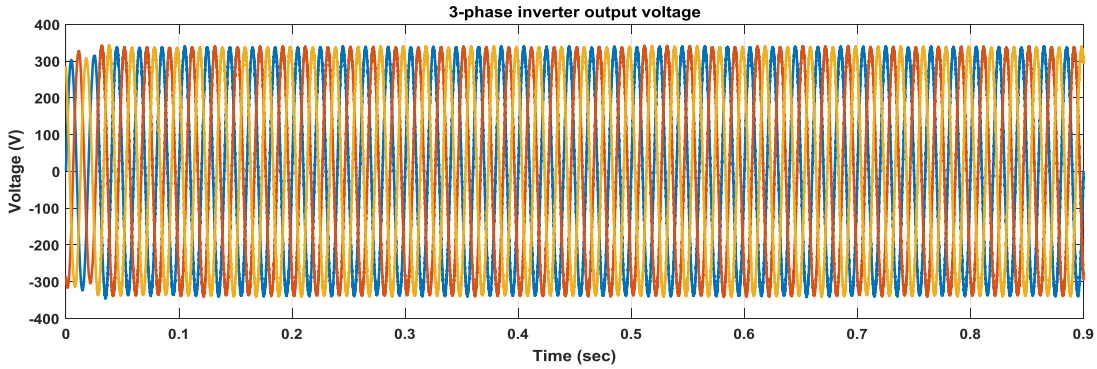

Figure 15:3-phase inverter output voltage

Figure 15 shows the inverter output AC voltage. The peak value of AC voltage is constant at 340V.

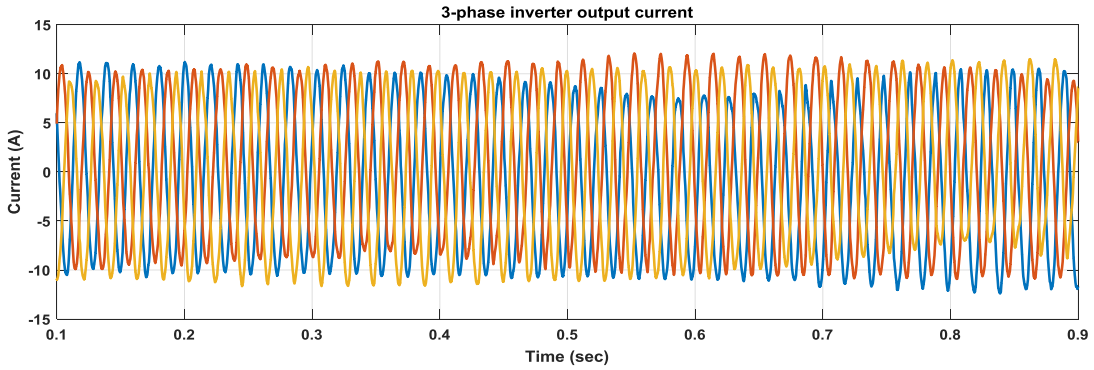

Figure 16:3-phase inverter output current

Figure 16 shows the inverter output 3- Phase current. The current and voltages are synchronized with the grid using the phase locked loop with current hysteresis control.

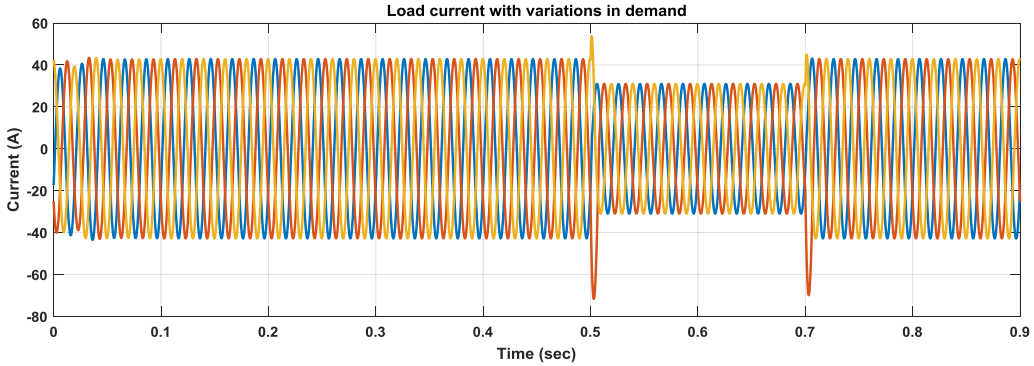

Figure 17: Load current with variations in demand

Figure 17 depicts the load current supplied by the system. This has been seen that the peak load current is reduced from 42 A to 32 A at 0.5 sec and further increased to 42 A at 0.7 sec with controlled oscillations in the system. This shows the enhanced dynamic stability of the proposed system under sudden change in loading conditions.

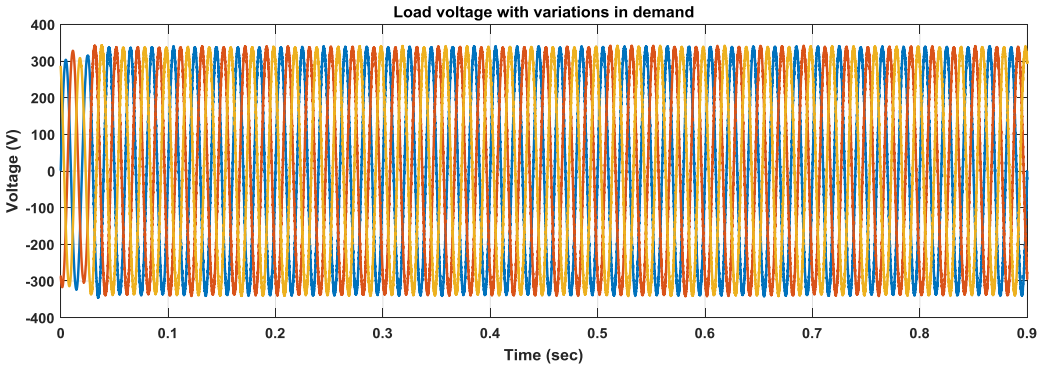

Figure 18: Load voltage with variations in demand

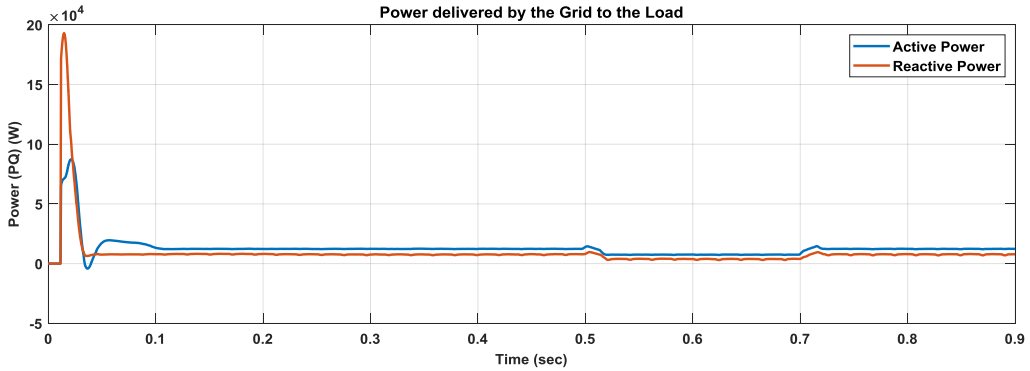

Figure 19 (a): Power delivered by the Grid to the Load

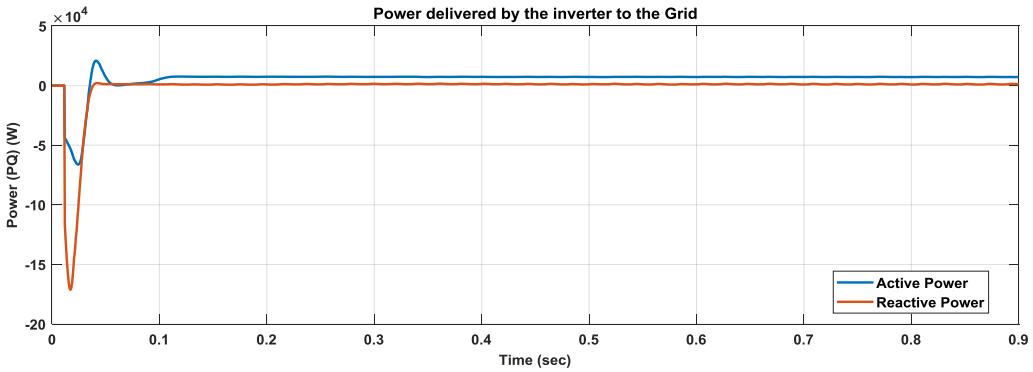

Figure 19(b) : Power delivered by the inverter to the Grid

Figure 18 shows the 3-phase voltage of the load. This has been seen that the voltage is constant without any fluctuations even in the presence of loading uncertainties. This shows the robustness of the system with proposed control scheme under the varying loading conditions. Figure 19(a) and 19(b) shows the power delivered by Grid to the R-L load and inverter to the grid respectively.

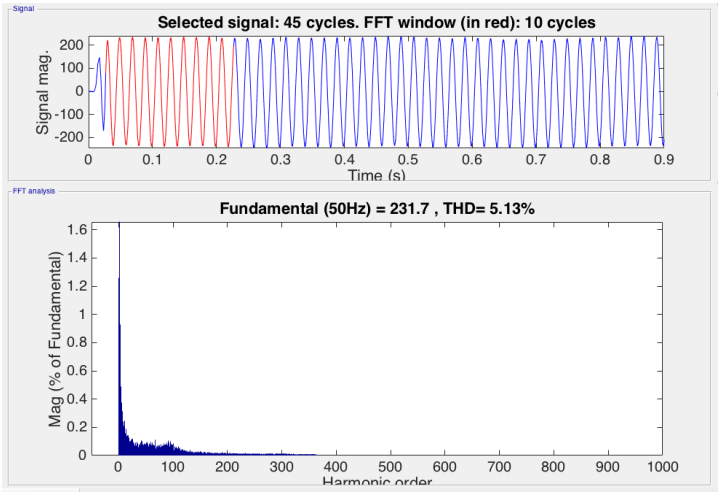

Figure 20(a) : THD level of inverter 3-phase voltage with conventional PID controller

The sudden switching of R-L load in the hybrid system may cause high frequency sinusoidal current/voltage harmonics in the system. The harmonic distortion present in current/voltage is measured by total harmonic distortion (THD). In this work, the THD is calculated for both voltage and current with conventional PID and GOA-PID controller and shown in tabular form in Table 3.

The THD level for inverter 3-phase output voltage with PID and GOA PID is provided in Figure 20(a) and 20(b) respectively. The THD value is reduced from 5.13% (with conventional PID) to 1.19 % (with GOA-PID) only. The THD level for inverter 3-phase output current with PID and GOA PID is shown in Figure 21(a) and 21(b) respectively. The THD level with conventional PID is 9.80% whereas the THD with GOA-PID is reduced to 5.53% only.

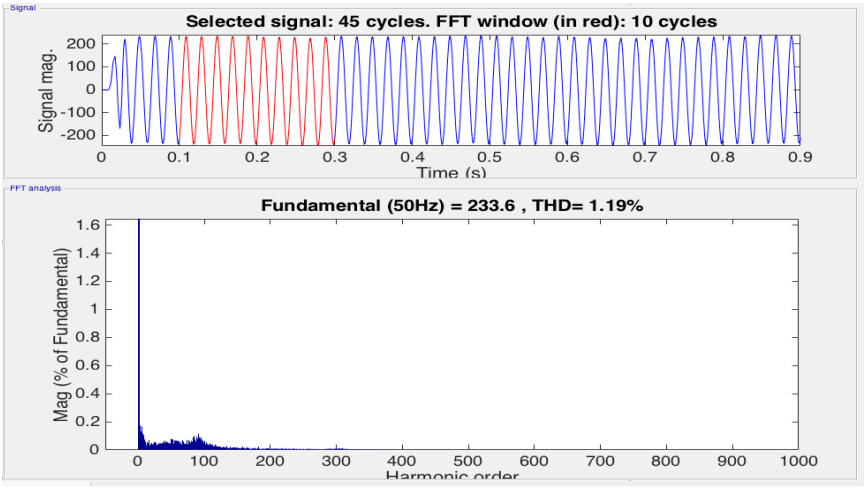

Figure 20(b) : THD level of inverter 3-phase voltage with GOA-PID controller

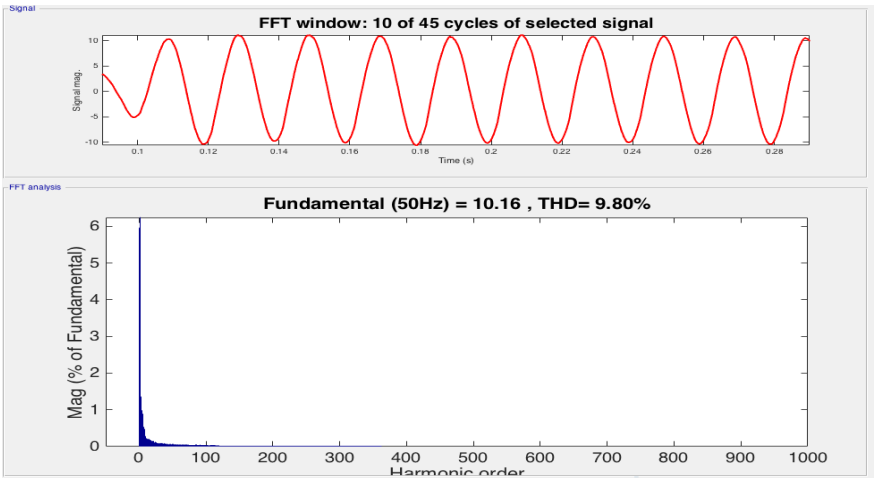

Figure 21(a) : THD level of inverter 3-phase current with conventional PID controller

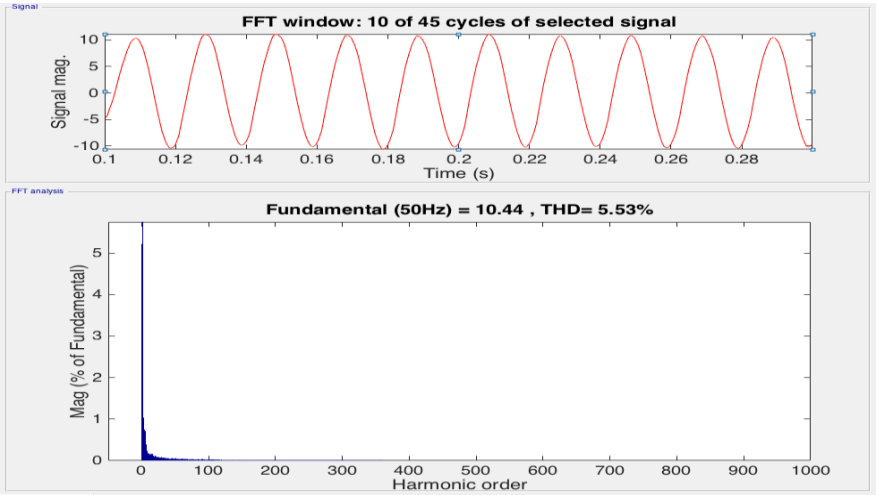

Figure 21(b) : THD level of inverter 3-phase current with GOA-PID controller

Therefore, the settling time, overshoot and THD values are improved with GOA optimized PID controller in comparison with conventional or manually tuned PID controller. Therefore, system performance as well as dynamic stability of the system is enhanced in presence of loading uncertainties.

Table 3 : Comparison of THD of Inverter voltages and currents with PID and GOA-PID

Parameter	With PID Controller (%)	With GOA-PIDController (%)
THD (voltage)	5.13	1.19
THD (current)	9.80	5.53

6. Conclusion

The continuous rise in power demand is unable to meet by conventional energy sources only. This requires exploring alternative sources of energy such as wind, solar and fuel cell. In this work, a hybrid power system model with solar, wind and fuel cells integrated with grid has been presented. The uncertainties in wind speed, solar radiation and loading are well tackled by Grasshopper tuned PID Controller. The computer simulation results show far better over shoot, THD levels of the voltage and current by GOA-PID control scheme in comparison with conventional PID controller. Thus, there is a remarkable improvement in power quality and dynamic stability of the system.

References

[1] Lalouni S and Rekioua D., "Modeling and simulation of a photovoltaic system using fuzzy logic controller", In: Proceedings - international conference on developments in eSystems engineering, DeSE, pp. 23-28, 2009.

[2] McGowan JG, Manwell JF, Avelar C and Warner CL.,"Hybrid wind/ PV/diesel hybrid power systems modeling and South American applications", Renewable energy. World Renew Energy Congr Colo USA, pp. 836-47, 1996.

[3] Yazic MS, Yavasoglu HA and Eroglu M., "A mobile off-grid platform powered with photovoltaic/wind/battery/fuel cell hybrid power

systems", Int J Hydrogen Energy, 38(26), pp. 11639-45, 2013.

[4] Castaneda M, Cano A, Jurado F, S ~ anchez H, Fern andez LM.,"Sizing optimization, dynamic modeling and energy management strategies of a stand-alone PV/hydrogen/ battery-based hybrid system", Int J Hydrogen Energy , 38(10), pp.3830-45, 2013.

[5] Abdelli R, Rekioua D, Rekioua T and Tounzi A.,"Improved direct torque control of an induction generator used in a wind conversion system connected to the grid", ISA Trans, vol. 52, pp. 525-38, 2013.

[6] Pourmousavi SA, Nehrir MH, Colson CM and Wang C. "Real-time energy management of a stand-alone hybrid windmicroturbine energy system using particle swarm optimization", IEEE Trans Sustain Energy,vol. 1(3), pp. 193-201, 2010.

[7] M.N. Eskander, T. F. El-Shatter and M.T. El-Hagry, "Energy Flow and Management of A Hybrid Wind/PV/Fuel Cell Generation System," Power Electronics Specialists Conference, vol. 1, pp. 347- 353, June 2002.

[8] Xin Wang, Yuvarajan, S. Lingling Fan., "MPPT control for a PMSG-based grid-tied wind generation system", IEEE Transactions on Energy Conversion, 2010.

[9] Yang Hongxing, Lu Lin and Zhou Wei. "A novel optimization sizing model for hybrid solar – wind power generation system", J Sol Energy, vol. 81(1), pp. 76-84, 2007.

[10] Mitchell K, Nagria M, Rizk J "Simulation and optimization of renewable energy systems" J Electric Power Syst ,vol. 27(3), pp. 177-188, 2005.

[11] Senjyu Tomonobu, Nakaji Toshiaki, Uezato Katsumi and Funabashi Toshihisa "A hybrid power system using alternative energy facilities in isolated island", IEEE Trans Energy Convers. , pp. 406-14, 2005.

[12] Islam Saiful and Belmans Ronnie, "Grid independent photovoltaic fuel cell hybrid system: design and control strategy", KIEEInt Trans Elect Mach Energy Convers Syst , pp. 399-404, 2005.

[13] Yang Hongxing, Lu Lin and Zhou Wei,"A novel optimization sizing model for hybrid solar–wind power generation system", J Sol Energy, vol. 81(1), pp. 76–84, 2007.

[14] Hoff Thomas E, Perez Richard, Margolis Robert M.,"Maximizing the value of customer-sited PV systems using storage and controls", J Sol Energy,, vol. 81(7), pp. 940–5, 2007.

[15] Billinton Roy and Karki Rajesh,"Capacity expansion of small isolated power systems using PV and wind energy". IEEE Trans Power Syst, vol. 6(4), pp. 892–7, 2001.

[16] Celik Ali Naci,"Techno-economic analysis of autonomous PV–wind hybrid energy systems using different sizing methods", J Energy Convers Manage, vol. 44(12), pp. 1951–68, 2003.

[17] Karki Rajesh and Billinton Roy,"Reliability/cost implications of PV and wind energy utilization in small isolated power systems". IEEE Trans Energy Convers, vol. 16(4), pp.368–73, 2001.

[18] Ahmed Nabil A and Miyatake Masafumi,"A stand-alone hybrid generation system combining solar photovoltaic and wind turbine with simple maximum power point tracking control" IEEE 5th international power electronics and motion control conference, 2006.

[19] Ayad Mohamed-Yacine, Pierfederici Serge, Rael Stephane and Davat Bernard,"Voltage regulated hybrid DC power source using supercapacitors as energy storage device". J Energy Convers Manage vol. 48(7), pp. 2196–2202, 2007.

[20] Rajashekara Kaushik,"Hybrid fuel-cell strategies for clean power generation". IEEE Trans Ind Appl, vol. 41(3), pp. 682–689, 2005.

[21] Ahmad Rouhani, Hossein Kord and Mahdi Mehrabi, "A Comprehensive Method for Optimum Sizing of Hybrid Energy Systems using Intelligence Evolutionary Algorithms", Indian Journal of Science and Technology, vol. 6 (6), pp. 4702-4712, 2013.

[22] Alireza Askarzadeh a, "Application of Ant Colony Optimization (ACO) for designing a hybrid system", International Journal of Engineering & Applied Sciences (IJEAS), vol.6, pp. 52-63, 2014.

[23] V.K.Tayal and J.S. Lather, "Reduced order H_∞ TCSC Controller & PSO Optimized Fuzzy PSS Design in Mitigating Small Signal Oscillations in a Wide Range," International Journal of Electric Power and Energy Systems (Elsevier), vol. 68, pp. 123–131, June 2015.

[24] V. K. Tayal and J. S. Lather, "PSO based Robust Fuzzy Power System Stabilizer Design for Single Machine Infinite Bus System", IEEE international Conference (INDICON), pp. 1-6, 2015.

[25] M.J. Khan and M.T. Iqbal, "Dynamic modeling and simulation of a small windfuel cell hybrid energy system", J. Renewable Energy, vol. 30 (3), pp. 421–439, 2005.

[26] H. De Battista, R.J. Mantz and F. Garelli, "Power conditioning for a windhydrogen energy system", J. Power Sources 155 (2), pp. 478–486.

[27] B. Delfino and F. Fornari, "Modeling and control of an integrated fuel cellwind turbine system", in: Proceedings of the IEEE PowerTech Conference, Bologna, vol. 2, pp. 6, 2003.
[28] E.S. Abdin, W. Xu, Control design and dynamic performance analysis of a wind turbine-induction generator unit, IEEE Trans. Energy Conversion 15 (1), pp. 91–96, 2000.
[29] S. Heier, "Grid Integration of Wind Energy Conversion Systems", John Wiley & Sons Ltd, New York, 1998.
[30] MATLAB SimPowerSystems for Use with Simulink User's Guide, Version 4.1.1, http://www.mathworks.com/access/helpdesk/help/pdf doc/ physmod/powersys/powersys.pdf.
[31] M. R. Patel, "Wind and Solar Power Systems". Boca Raton, FL: CRC Press, 1999.
[32] Ø. Ulleberg and S. O. Mørner, "TRNSYS simulation models for solar- hydrogen systems," Solar Energy, vol. 59, no. 4–6, pp. 271–279, 1997.
[33] E. S. Abdin, A. M. Osheiba, and M. M. Khater, "Modeling and optimal controllers design for a stand-alone photovoltaic-diesel generating unit," IEEE Trans. Energy Convers., vol. 14, no. 3, pp. 560–565, Sep. 1999.
[34] Ahmed Nabil A., "Computational modeling and polarization characteristics of proton exchange membrane fuel cell with evaluation of the interface systems", Eur Power Electron J, 18(1), 2008.
[35] Uzunoglu M and Alam MS., "Dynamic Modeling, Design and simulation of a PEM fuel cell/ultra-capacitor hybrid system for vehicular applications". J Energy Convers Manage , 48(5), pp. 1544–53.
[36] Kelley TR, "Optimization, an important stage of engineering design", Technol Teacher, pp. 18-23, 2008.
[37] Coello CA, "Theoretical and numerical constraint-handling techniques used with evolutionary algorithms: A survey of the state of the art", Comput Meth Appl Mech Eng 191,pp. 1245-1287, 2002.
[38] Marler RT and Arora JS, "Survey of multi-objective optimization methods for engineering", Struct Multidiscipl Optim 26, pp. 369-95, 2004.
[39] Simpson SJ, McCaffery A and Haegele BF "A behavioural analysis of phase change in the desert locust", Biol Rev 74, pp. 461-80, 1999.
[40] Rogers SM, Matheson T, Despland E, Dodgson T, Burrows M, et al., "Mechanosensory-induced behavioural gregarization in the desert locust Schistocerca gregaria". J Exp Biol 206, pp. 3991-4002, 2003.
[41] Topaz CM, Bernoff AJ, Logan S and Toolson W, "A model for rolling swarms of locusts", Eur Phys J Special Top 157,pp. 93-109, 2008.
[42] Abhishek G Neve, Ganesh M Kakandikar and Omkar Kulkarni "Application of Grasshopper Optimization Algorithm for Constrained and Unconstrained Test Functions" Neve et al., Int J Swarm Intel Evol Comput , 2017.
[43] Saremi S, Mirjalili S and Lewis A,"Grasshopper optimisation algorithm:Theory and application". Adv Eng Soft 105, pp. 30-47, 2017.